Oct 19th, 12:00 AM

# T-joints Made of Rectangular Tubes

Ben Kato

Isao Nishiyama

# T-JOINTS MADE OF RECTANGULAR TUBES

By Ben Kato[1] and Isao Nishiyama[2]

## 1. INTRODUCTION

Different types of welded joints made of rectangular or square hollow sections were investigated by several researchers. The b/B-ratio (the ratio of brace flange width to chord flange width) of these joints tested were relatively small and the maximum strengths of these joints were governed by the local flexural failure of flanges of chord members. For these joints, the empirical formulae for the prediction of yield strength and thus the practical design formulae were already established on the basis of sufficient number of test results (1,4,6)[3]. Theoretical prediction making use of the yield-line theory is also promising for this type of joints.

It is expected that the joint efficiency may increase with the increase of b/B-ratio to a certain extent. When this b/B-ratio arrives at a certain limit, the mode of failure will convert from the chord flange failure type to the chord web failure type. As for the maximum strengths of joints with large b/B-ratio, the failure mode of which is the chord web failure type (web-crippling type), no systematic research was carried out and thus no practically useful information was obtained as yet.

In this research, the ultimate strengths of T-joints made of rectangular hollow section members with large b/B-ratio (the width of brace member b is close to that of chord member B) were investigated experimentally.

Another problem is the local buckling strength of brace members. Brace members in T-joints are supported by the flanges of chord members at one end. Since the flexural rigidities of a chord flange are different each other in longitudinal and transverse directions, axial stresses in two walls of a brace member perpendicular each other may show some difference. As b/B-ratio increases, this difference will become significant.

The effect of such anisotropic supporting foundations on the local buckling strength of the brace members were also investigated.

The rectangular hollow sections used in this experiments were manufactured by cold-forming, and in order to examine the possible effects of cold-working and residual stresses on the strengths of joints, some specimens were fabricated using stress-relieved rectangular hollow section members and tested.

---

(footnote)
[1]Professor of the University of Tokyo, Japan.
[2]Graduate Student, the University of Tokyo, Japan.
[3]Numerals in parentheses refer to corresponding items in the APPENDIX.--REFERENCES.

## 2. TEST SPECIMENS

The shape and the geometrical symbols are shown in Fig.1. In the figure B = flange width of chord member; H = web depth of chord member; $t_c$ = plate thickness of chord member; b = flange width of brace member; w = web depth of brace member; $t_b$ = plate thickness of brace member; r = $2t_c$ = radius of curvature on the outer surface of the rectangular hollow section; L = span length of chord member; and h = length of brace member.

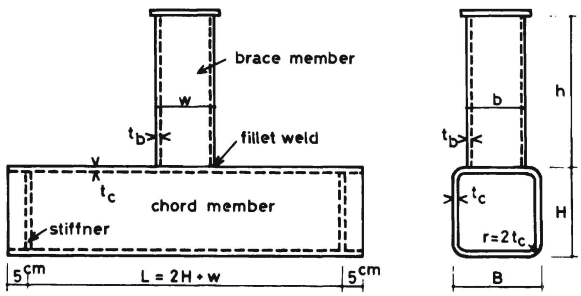


FIG.1.-TEST SPECIMEN

The span length of chord member (L) must not only be short enough to prevent the premature flexural failure of chord member as a beam but also be long enough to avoid the stress disturbance and truss action caused by the reactions of end supports. So as to satisfy these conditions, the span length of chord member is decided to be 2H+w (3). The length of brace member is decided to be the larger of 3b and 3w, which is the same length as the corresponding stub column.

The dimensions of the specimens are all listed in Table 1. The total number of specimens are fifty and six of them are to examine the effects of cold-working and residual stresses on the strengths of the joints and they are identified by the primes on their specimen number (see column 1). The main parameters are b/B-ratio and $\gamma = H/t_c$ = depth-to-thickness ratio of chord member. The size of the fillet weld is equal to the larger wall thickness of the sections jointed.

## 3. MECHANICAL PROPERTIES

The base material of the cold-formed rectangular hollow sections is the mild steel grade SS41 according to the Japanese Industrial Standard (JIS) with a specified minimum yield stress $\sigma_{YJIS}$ = 235N/mm$^2$ and a specified minimum tensile stress $\sigma_{TJIS}$ = 402N/mm$^2$.

The measured mechanical properties of the material are listed in Table 2. For all the sections used, the yield stress and the maximum or tensile stress were determined by stub column compression tests and coupon tensile tests. In the table A = sectional area of rectangular hollow section; $P_{ms}$ = maximum load of stub column; $\sigma_{ms} = P_{ms}/A$ = maximum stress of stub column; $P_{ys}$ = yield load of stub column; $\sigma_{ys} = P_{ys}/A$ = yield stress of stub column; $\sigma_T$ = tensile

TABLE 1.-TEST SPECIMEN

| Specimen number | Chord member | | | Brace member | | | b/B | γ |
|---|---|---|---|---|---|---|---|---|
| | B mm | H mm | $t_c$ mm | b mm | w mm | $t_b$ mm | | |
| (1) | (2) | (3) | (4) | (5) | (6) | (7) | (8) | (9) |
| 1 | 127 | 127 | 7.9 | 102 | 102 | 6.4 | 0.80 | 16.0 |
| 1' | 127 | 127 | 7.9 | 102 | 102 | 6.4 | 0.80 | 16.0 |
| 2 | 150 | 150 | 6.0 | 125 | 125 | 6.0 | 0.83 | 25.0 |
| 2' | 150 | 150 | 6.0 | 125 | 125 | 6.0 | 0.83 | 25.0 |
| 3 | 200 | 200 | 6.0 | 178 | 178 | 12.7 | 0.89 | 33.3 |
| 4 | 127 | 127 | 3.0 | 102 | 102 | 6.4 | 0.80 | 41.7 |
| 5 | 127 | 127 | 3.0 | 102 | 51 | 6.4 | 0.80 | 41.7 |
| 6 | 127 | 127 | 3.0 | 102 | 152 | 6.4 | 0.80 | 41.7 |
| 7 | 127 | 127 | 3.0 | 102 | 203 | 6.4 | 0.80 | 41.7 |
| 8 | 203 | 203 | 4.8 | 178 | 178 | 12.7 | 0.88 | 42.7 |
| 9 | 102 | 102 | 2.4 | 76 | 76 | 4.8 | 0.75 | 42.1 |
| 10 | 250 | 150 | 9.0 | 200 | 200 | 9.0 | 0.80 | 16.7 |
| 11 | 150 | 150 | 6.0 | 100 | 100 | 6.0 | 0.67 | 25.0 |
| 12 | 200 | 200 | 6.0 | 150 | 150 | 6.0 | 0.75 | 33.0 |
| 13 | 250 | 250 | 6.0 | 200 | 200 | 9.0 | 0.80 | 41.7 |
| 14 | 300 | 300 | 6.0 | 250 | 250 | 6.0 | 0.83 | 50.0 |
| 15 | 250 | 150 | 9.0 | 178 | 178 | 12.7 | 0.71 | 16.7 |
| 16 | 150 | 150 | 6.0 | 75 | 75 | 3.2 | 0.50 | 25.0 |
| 17 | 200 | 200 | 6.0 | 125 | 125 | 6.0 | 0.63 | 33.3 |
| 17' | 200 | 200 | 6.0 | 125 | 125 | 6.0 | 0.63 | 33.3 |
| 18 | 250 | 250 | 6.0 | 178 | 178 | 12.7 | 0.71 | 41.7 |
| 19 | 229 | 178 | 4.6 | 102 | 102 | 6.4 | 0.44 | 38.9 |
| 20 | 178 | 178 | 12.7 | 50 | 50 | 2.3 | 0.28 | 14.0 |
| 21 | 254 | 254 | 9.5 | 127 | 127 | 6.4 | 0.50 | 26.7 |
| 22 | 178 | 178 | 12.7 | 127 | 127 | 6.4 | 0.71 | 14.0 |
| 23 | 127 | 127 | 7.9 | 102 | 102 | 4.8 | 0.80 | 16.0 |
| 24 | 150 | 150 | 6.0 | 127 | 127 | 6.4 | 0.85 | 25.0 |
| 25 | 250 | 250 | 6.0 | 75 | 75 | 2.3 | 0.30 | 41.7 |
| 26 | 150 | 150 | 6.0 | 75 | 75 | 2.3 | 0.50 | 25.0 |
| 27 | 150 | 150 | 6.0 | 102 | 102 | 3.2 | 0.68 | 25.0 |
| 28 | 127 | 127 | 7.9 | 102 | 102 | 3.2 | 0.80 | 16.0 |
| 29 | 89 | 89 | 6.4 | 75 | 75 | 2.3 | 0.84 | 14.0 |
| 30 | 89 | 89 | 6.4 | 75 | 45 | 2.3 | 0.84 | 14.0 |
| 31 | 89 | 89 | 6.4 | 75 | 125 | 2.3 | 0.84 | 14.0 |
| 32 | 350 | 350 | 12.0 | 102 | 102 | 2.4 | 0.29 | 29.2 |
| 33 | 254 | 254 | 9.5 | 127 | 127 | 3.0 | 0.50 | 26.7 |
| 33' | 254 | 254 | 9.5 | 127 | 127 | 3.0 | 0.50 | 26.7 |
| 34 | 178 | 178 | 12.7 | 127 | 127 | 3.0 | 0.71 | 14.0 |
| 35 | 127 | 127 | 7.9 | 102 | 102 | 2.4 | 0.80 | 16.0 |
| 36 | 254 | 254 | 9.5 | 203 | 203 | 4.8 | 0.80 | 26.7 |
| 36' | 254 | 254 | 9.5 | 203 | 203 | 4.8 | 0.80 | 26.7 |
| 37 | 150 | 150 | 6.0 | 127 | 127 | 3.0 | 0.85 | 25.0 |
| 38 | 150 | 150 | 6.0 | 127 | 51 | 3.0 | 0.85 | 25.0 |
| 39 | 300 | 300 | 12.0 | 250 | 250 | 6.0 | 0.83 | 25.0 |
| 40 | 350 | 350 | 12.0 | 102 | 102 | 2.1 | 0.29 | 29.2 |
| 41 | 203 | 203 | 9.5 | 102 | 102 | 2.1 | 0.50 | 21.3 |
| 41' | 203 | 203 | 9.5 | 102 | 102 | 2.1 | 0.50 | 21.3 |
| 42 | 150 | 150 | 6.0 | 102 | 102 | 2.1 | 0.68 | 25.0 |
| 43 | 127 | 127 | 7.9 | 102 | 102 | 2.1 | 0.80 | 16.0 |
| 44 | 350 | 350 | 12.0 | 300 | 300 | 6.0 | 0.86 | 29.2 |

strength of test coupon; and $\sigma_y$ = yield stress of test coupon.

The yield stress was determined on the basis of 0.2% offset value. For stress-relieved materials, which had shown the sharp yielding, the lower yield point was used. The length of the stub column is 3b or 3w which is larger. Specimens for which no yield stresses were shown in the table had buckled in elastic region. The tensile coupons of the hollow sections were taken longitudinally from the center of the flat parts. Three coupons were taken from

TABLE 2.-MECHANICAL PROPERTIES

| Tube number | Section | A | Stub column test | | | | Coupon test | |
|---|---|---|---|---|---|---|---|---|
| | b.B x w.H x $t_b$.$t_c$ mm | $cm^2$ | $P_{ms}$ kN | $\sigma_{ms}$ $N/mm^2$ | $P_{ys}$ kN | $\sigma_{ys}$ $N/mm^2$ | $\sigma_T$ $N/mm^2$ | $\sigma_y$ $N/mm^2$ |
| (1) | (2) | (3) | (4) | (5) | (6) | (7) | (8) | (9) |
| m 1 | 350 x 350 x 12.0 | 156.1 | 4923 | 316 | 4815 | 309 | 409 | 264 |
| m 2 | 300 x 300 x 12.0 | 134.5 | 5560 | 414 | 5148 | 382 | 460 | 353 |
| m 3 | 254 x 254 x 9.5 | 90.8 | 3932 | 432 | 3599 | 396 | 481 | 380 |
| m 3' | 254 x 254 x 9.5 | 90.8 | 3481 | 383 | - | - | 477 | 351 |
| m 4 | 178 x 178 x 12.7 | 79.7 | 3801 | 477 | 3158 | 396 | 446 | 380 |
| m 5 | 203 x 203 x 9.5 | 71.5 | 3491 | 488 | 3089 | 432 | 483 | 429 |
| m 5' | 203 x 203 x 9.5 | 71.5 | 2862 | 400 | 2824 | 395 | 486 | 393 |
| m 6 | 300 x 300 x 6.0 | 69.6 | 1800 | 259 | - | - | 444 | 368 |
| m 7 | 200 x 200 x 9.0 | 66.7 | 2962 | 444 | 2677 | 402 | 466 | 414 |
| m 8 | 250 x 150 x 9.0 | 66.7 | 2736 | 411 | 2569 | 385 | 450 | 387 |
| m 9 | 250 x 250 x 6.0 | 57.6 | 1922 | 333 | - | - | 490 | 400 |
| m 10 | 200 x 200 x 6.0 | 45.6 | 1704 | 374 | - | - | 459 | 368 |
| m 10' | 200 x 200 x 6.0 | 45.6 | 1608 | 352 | - | - | 456 | 333 |
| m 11 | 152 x 152 x 7.9 | 44.2 | 2230 | 504 | 1804 | 408 | 469 | 407 |
| m 12 | 203 x 203 x 4.8 | 37.2 | 1158 | 311 | - | - | 442 | 348 |
| m 12' | 203 x 203 x 4.8 | 37.2 | 1232 | 331 | - | - | 427 | 312 |
| m 13 | 127 x 127 x 7.9 | 36.2 | 1650 | 456 | 1446 | 400 | 453 | 404 |
| m 13' | 127 x 127 x 7.9 | 36.2 | 1671 | 462 | 1353 | 374 | 446 | 342 |
| m 14 | 102 x 203 x 6.4 | 36.1 | 1549 | 430 | 1503 | 417 | 546 | 420 |
| m 15 | 229 x 178 x 4.6 | 35.8 | 1173 | 328 | - | - | 456 | 375 |
| m 16 | 150 x 150 x 6.0 | 33.6 | 1309 | 389 | 1216 | 362 | 431 | 366 |
| m 16' | 150 x 150 x 6.0 | 33.6 | 1103 | 329 | 1090 | 325 | 431 | 328 |
| m 17 | 127 x 127 x 6.4 | 29.6 | 1352 | 457 | 1226 | 414 | 505 | 446 |
| m 18 | 102 x 152 x 6.4 | 29.6 | 1234 | 417 | 1147 | 387 | 446 | 388 |
| m 19 | 125 x 125 x 6.0 | 27.6 | 1182 | 428 | 1054 | 381 | 462 | 383 |
| m 19' | 125 x 125 x 6.0 | 27.6 | 985 | 356 | 946 | 342 | 448 | 340 |
| m 20 | 102 x 102 x 6.4 | 23.2 | 1089 | 470 | 986 | 426 | 486 | 431 |
| m 20' | 102 x 102 x 6.4 | 23.2 | 1053 | 455 | 908 | 392 | 473 | 379 |
| m 21 | 100 x 100 x 6.0 | 21.6 | 1102 | 510 | 971 | 449 | 492 | 424 |
| m 22 | 89 x 89 x 6.4 | 19.9 | 890 | 447 | 726 | 364 | 471 | 403 |
| m 23 | 102 x 102 x 4.8 | 17.9 | 809 | 453 | 714 | 400 | 493 | 423 |
| m 24 | 102 x 51 x 6.4 | 16.7 | 852 | 510 | 741 | 444 | 498 | 431 |
| m 25 | 127 x 127 x 3.0 | 14.9 | 496 | 333 | - | - | 469 | 382 |
| m 25' | 127 x 127 x 3.0 | 14.9 | 513 | 345 | - | - | 450 | 343 |
| m 26 | 76 x 76 x 4.8 | 13.0 | 645 | 495 | 563 | 432 | 511 | 452 |
| m 27 | 102 x 102 x 3.2 | 12.2 | 471 | 384 | 459 | 375 | 456 | 393 |
| m 28 | 127 x 51 x 3.0 | 10.2 | 411 | 402 | - | - | 514 | 426 |
| m 29 | 75 x 75 x 3.2 | 9.9 | 367 | 370 | 333 | 336 | 471 | 390 |
| m 30 | 102 x 102 x 2.4 | 9.4 | 257 | 273 | - | - | 453 | 369 |
| m 31 | 75 x 125 x 2.3 | 8.9 | 221 | 249 | - | - | 463 | 359 |
| m 32 | 102 x 102 x 2.1 | 8.3 | 225 | 272 | - | - | 452 | 366 |
| m 32' | 102 x 102 x 2.1 | 8.3 | 232 | 280 | - | - | 443 | 347 |
| m 33 | 75 x 75 x 2.3 | 6.6 | 209 | 319 | 204 | 311 | 445 | 358 |
| m 34 | 75 x 45 x 2.3 | 5.2 | 188 | 364 | 184 | 356 | 461 | 396 |
| m 35 | 50 x 50 x 3.0 | 4.3 | 150 | 353 | 142 | 333 | 403 | 357 |

one section (excluding the welded side) and the average value of these three coupon tests was listed in the table.

As seen in the table, about 10% reduction of the yield stress was observed by applying the stress-relieving (annealing).

## 4. LOADING AND MEASUREMENTS

The test set up was shown in Fig.2. As shown in the figure, one end of the chord member was pin-supported and another end was supported by roller. And free end of the brace member was compressed by testing machine.

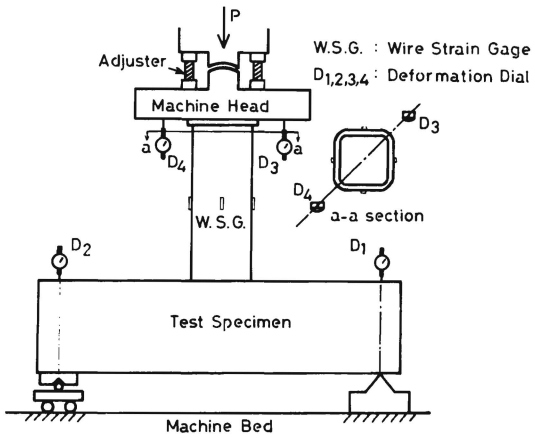


FIG.2.-LOADING AND MEASUREMENTS

Firstly, in order to achieve the concentric loading, the adjustment of the set up of a test specimen was made keeping the head of the testing machine free to rotate. Loading condition was monitored by the readings of the four wire strain gages mounted at each side of the brace member. After achieving the concentric loading condition, the head of the testing machine was fixed and the load was applied monotonically up to the failure of the specimen.

From the readings of the four deformation dials shown in the figure, the following quantity $\Delta$ was calculated.

$$\Delta = \left( \frac{D_1+D_2}{2} + \frac{D_3+D_4}{2} \right) \qquad \ldots\ldots\ldots \quad (1)$$

This quantity is not the genuine local deformation of the joint but it includes the axial shortening of the brace member and also the bending deflection of the chord member as a beam. But this quantity $\Delta$ was chosen as a measure of deformation in this research.

## 5. TEST RESULTS

### 5.1. FAILURE MODES

Configurations of all test specimens at the ultimate state can be categorized into three principal modes and two combination modes as shown in Fig.3.

The characteristic feature of these failure modes are:

M1: web-crippling failure (chord web failure);
M2: flexural failure of chord flange (chord flange failure);
M3: plate buckling (local buckling) of brace member;
M4(M1+M2): combined mode of web-crippling and flange yielding of chord

member; and

M5(M2+M3): combined mode of flange yielding of chord member and local buckling of brace member (specimens whose brace buckled after very large amount of inelastic deformation by flange yielding were classified into M2).

Failure modes of all test specimens are identified according to this classification in Table 3 (column 9) which summarized all test results.

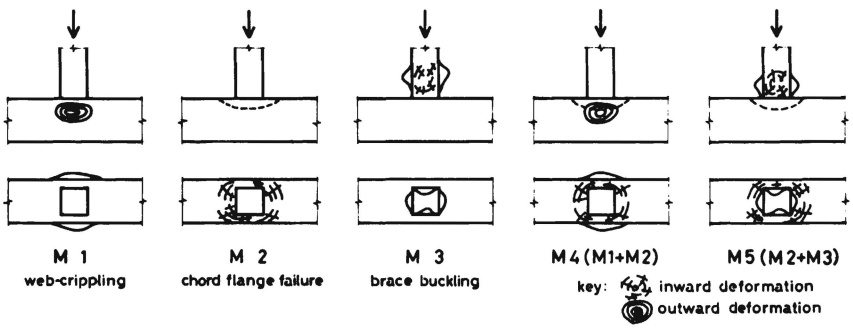


FIG.3.-TYPICAL FAILURE MODES

## 5.2. LOAD-DEFORMATION CURVES

Load-deformation curves of all test specimens are shown in Fig.4, where applied load P is taken in vertical axis and $\Delta$ calculated by Eq.1 is taken in horizontal axis.

In these curves, the characteristic damage points observed in the course of loading were shown by the following marks:

▽-mark: the point when the web-crippling of a chord member became significant;

▼-mark: the point when the flange yielding of a chord member became significant;

x-mark: the point when the local buckling of a brace member took place; and

o-mark: the general yield load of a specimen.

These load-deformation curves can also be categorized into five groupes and can be schematically depicted as shown in Fig.5. As seen in the figure, these characteristic load-deformation curves have a good correlation with the characterized failure modes and it can be explained as followings:

M1: when the web-crippling of chord member takes place, the load carrying capacity of the chord member as a beam starts to decrease, which leads the gradual downward slope of the load-deformation curve;

M2: when the yielding of chord flange takes place due to bending, the load-deformation curve shows a clear knee, but the load carrying capacity of the specimen continues to increase due to the effect of membrane action of the flange;

M3: when the local buckling of brace member takes place, the load drops

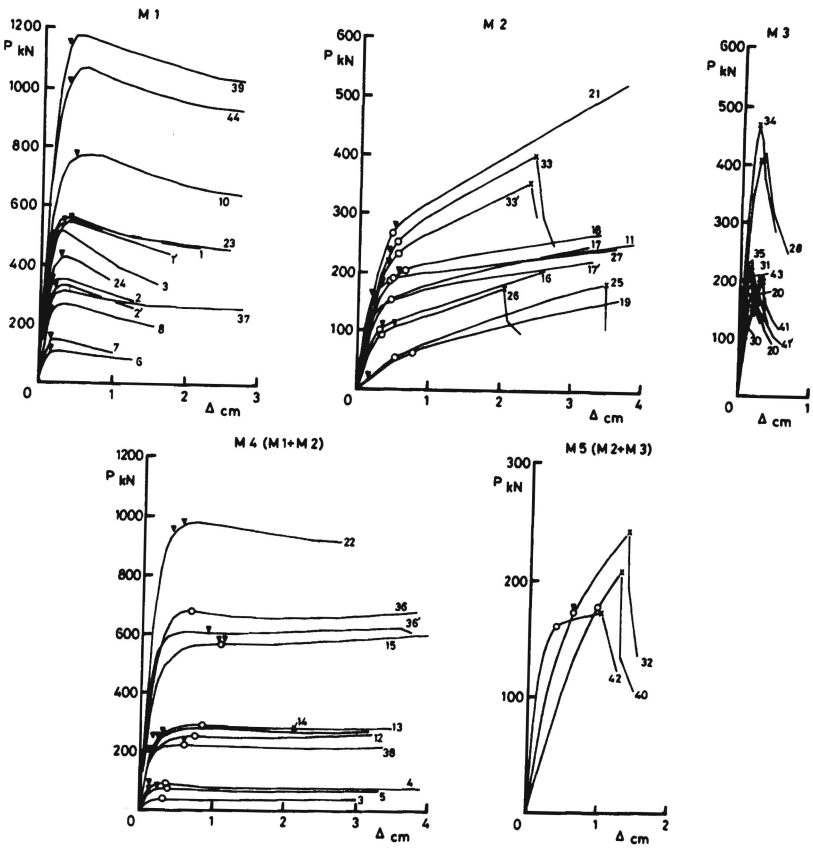


FIG.4.-LOAD-DEFORMATION CURVES


FIG.5.-CHARACTERIZED LOAD-DEFORMATION CURVES

quite suddenly which is common phenomenon with buckling.

M4: this is the combined failure of web-crippling and flange yielding of chord member, and the load-deformation curve also shows the combined shape of M1 and M2, namely the load carrying capacity continues to keep its level due to the effect of membrane action after web-crippling took place; and

M5: this is the combined failure of chord flange yielding and brace buckling. After being subjected to some amount of plastic deformation due to the yielding of chord flange, the local buckling of brace member takes place and the load drops suddenly.

## 5.3. MAXIMUM LOADS AND YIELD LOADS

Test results are summarized in Table 3, which includes the following items:

column 1: the specimen number was accorded to the number shown in Table 1;

column 2: $b/B$ = the ratio of brace flange width to chord flange width (which is already included in Table 1);

column 3: $e = (B-b)/2$ = distance between surfaces of webs of chord and brace members;

column 4: $\gamma = H/t_c$ = width-to-thickness ratio of chord web (which is already included in Table 1);

column 5: $P_m$ = the measured maximum loads of test specimens (In most of the M2-type of specimens, loading was stopped before they reached the maximum loads due to the excessive deflection, and for these specimens the loads at the termination of loading were shown and they are checked by *-mark);

column 6: $P_y$ = the measured general yield loads of test specimens;

column 7: $P_{ms}$ = stub column buckling load. Local buckling loads of stub columns which have the same dimension as the corresponding brace members of test specimens are already available in Table 2, and these values can be compared with $P_m$ for M3 and M5-types of specimens;

column 8: $P_{fy}$ = flange yield load according to the yield-line theory. Test results are compared with this theoretical prediction and some discussion will be made in section 6.2.; and

column 9: corresponding failure modes (M1 through M5).

# 6. DISCUSSION OF THE TEST RESULTS

## 6.1. RELATION BETWEEN FAILURE MODE AND GEOMETRY

There are some interaction between flange yielding and brace buckling in M5-type of specimens, but some specimens whose brace buckling were preceded to the substantial flange yielding can be considered to be M3-type and others whose brace buckling had taken place after substantial flange yielding were observed can be considered to be M2-type, and thus M5-type can be dissolved from the strength viewpoint.

The load carrying capacity of M1-type of specimens is governed by web-crippling of chord webs, and that of M2-type of specimens is governed by the flexural yielding of chord flanges and M4-type of specimens are located in

TABLE 3.-TEST RESULTS

| Specimen number | Parameters | | | Test loads | | Reference loads | | Failure mode |
|---|---|---|---|---|---|---|---|---|
| | b/B | e mm | γ | $P_m$ kN | $P_y$ kN | $P_{ms}$ kN | $P_{fy}$ kN | |
| (1) | (2) | (3) | (4) | (5) | (6) | (7) | (8) | (9) |
| 1 | 0.80 | 12.7 | 16.0 | 565 | - | 1089 | - | M1 |
| 1' | 0.80 | 12.7 | 16.0 | 541 | - | 1053 | - | M1 |
| 2 | 0.83 | 12.5 | 25.0 | 353 | - | 1182 | 2558 | M1 |
| 2' | 0.83 | 12.5 | 25.0 | 332 | - | 985 | 2292 | M1 |
| 3 | 0.89 | 11.1 | 33.3 | 514 | - | 3801 | - | M1 |
| 4 | 0.80 | 12.7 | 41.7 | 88 | - | 1089 | 132 | M4 |
| 5 | 0.80 | 12.7 | 41.7 | 74* | 73 | 852 | 147 | M4 |
| 6 | 0.80 | 12.7 | 41.7 | 111 | - | 1234 | 143 | M1 |
| 7 | 0.80 | 12.7 | 41.7 | 148 | - | 1549 | 207 | M1 |
| 8 | 0.88 | 12.7 | 42.7 | 270 | - | 3801 | 1496 | M1 |
| 9 | 0.75 | 12.7 | 42.1 | 45* | 40 | 645 | 60 | M4 |
| 10 | 0.80 | 25.0 | 16.7 | 771 | - | 2962 | 2183 | M1 |
| 11 | 0.67 | 25.0 | 25.0 | 258* | 192 | 1102 | 246 | M2 |
| 12 | 0.75 | 25.0 | 33.0 | 262* | 250 | 1309 | 283 | M4 |
| 13 | 0.80 | 25.0 | 41.7 | 288 | - | 2962 | 428 | M4 |
| 14 | 0.83 | 25.0 | 50.0 | 281 | - | 1922 | 498 | M4 |
| 15 | 0.71 | 36.1 | 16.7 | 608* | 563 | 3801 | 747 | M4 |
| 16 | 0.50 | 37.5 | 25.0 | 208* | 102 | 367 | 135 | M2 |
| 17 | 0.63 | 37.5 | 33.3 | 248* | 154 | 1182 | 178 | M2 |
| 17' | 0.63 | 37.5 | 33.3 | 223* | 153 | 985 | 161 | M2 |
| 18 | 0.71 | 36.1 | 41.7 | 270* | 202 | 3801 | 247 | M2 |
| 19 | 0.44 | 63.5 | 38.9 | 157* | 63 | 1089 | 62 | M2 |
| 20 | 0.28 | 63.9 | 14.0 | 150 | - | 150 | 407 | M3 |
| 21 | 0.50 | 63.5 | 26.7 | 712 | 263 | 1352 | 320 | M2 |
| 22 | 0.71 | 25.4 | 14.0 | 965 | - | 1352 | 3743 | M4 |
| 23 | 0.80 | 12.7 | 16.0 | 548 | - | 809 | - | M1 |
| 24 | 0.85 | 11.5 | 25.0 | 430 | - | 1352 | - | M1 |
| 25 | 0.30 | 87.5 | 41.7 | 184 | 54 | 209 | 90 | M2 |
| 26 | 0.50 | 37.5 | 25.0 | 174 | 94 | 209 | 127 | M2 |
| 27 | 0.68 | 24.2 | 25.0 | 253* | 189 | 471 | 281 | M2 |
| 28 | 0.80 | 12.7 | 16.0 | 422 | - | 471 | - | M3 |
| 29 | 0.84 | 7.0 | 14.0 | 197 | - | 209 | - | M3 |
| 30 | 0.84 | 7.0 | 14.0 | 185 | - | 188 | - | M3 |
| 31 | 0.84 | 7.0 | 14.0 | 216 | - | 221 | - | M3 |
| 32 | 0.29 | 124.2 | 29.2 | 242 | 172 | 257 | 228 | M5 |
| 33 | 0.50 | 63.5 | 26.7 | 398 | 247 | 496 | 326 | M2 |
| 33' | 0.50 | 63.5 | 26.7 | 356 | 230 | 513 | 301 | M2 |
| 34 | 0.71 | 25.4 | 14.0 | 469 | - | 496 | 2516 | M3 |
| 35 | 0.80 | 12.7 | 16.0 | 233 | - | 257 | - | M3 |
| 36 | 0.80 | 25.4 | 26.7 | 706* | 668 | 1158 | 1280 | M4 |
| 36' | 0.80 | 25.4 | 26.7 | 619 | 598 | 1232 | 1182 | M4 |
| 37 | 0.85 | 11.5 | 25.0 | 316 | - | 496 | - | M1 |
| 38 | 0.85 | 11.5 | 25.0 | 225 | - | 411 | 1397 | M4 |
| 39 | 0.83 | 25.0 | 25.0 | 1172 | - | 1922 | - | M1 |
| 40 | 0.29 | 124.2 | 29.2 | 208 | 177 | 225 | 228 | M5 |
| 41 | 0.50 | 50.8 | 21.3 | 208 | - | 225 | 382 | M3 |
| 41' | 0.50 | 50.8 | 21.3 | 200 | - | 232 | 351 | M3 |
| 42 | 0.68 | 24.2 | 25.0 | 173 | 161 | 225 | 228 | M5 |
| 43 | 0.80 | 12.7 | 16.0 | 213 | - | 225 | - | M3 |
| 44 | 0.86 | 25.0 | 29.2 | 1065 | - | 1880 | 2905 | M1 |

between M1 and M2, but as far as the maximum load is concerned M4-type could be included in M1-type.

As the result of various survey, it is found that one of the most influential parameter on the change of failure mode is eccentricity e, and the relation between failure modes and eccentricity e is surveyed in Fig.6. From this figure the critical eccentricity seems to be about 30mm.

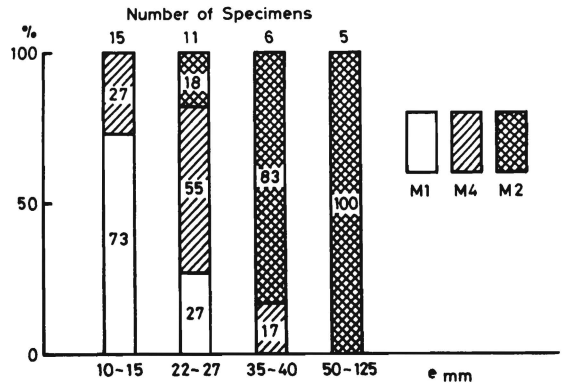


FIG.6.-RELATION BETWEEN FAILURE MODES AND ECCENTRICITY

6.2. YIELD STRENGTH OF CHORD FLANGE

The yield load of chord flange can be predicted by making use of the yield-line theory (2). Assuming the yield-lines in a joint as shown in Fig.7, the yield load can be expressed as follows:

$$P_{fy} = m_p\left(16\sqrt{\frac{B'}{B'-b'}} + \frac{8w'}{B'-b'}\right) \qquad \ldots\ldots\ldots (2)$$

in which $m_p = t_c^2\sigma_y/4$ = full plastic moment of flange plate per unit width, $\sigma_y$ is the tensile yield stress measured by coupon test; $B' = B-(4-1.5\sqrt{2})t_c$ =

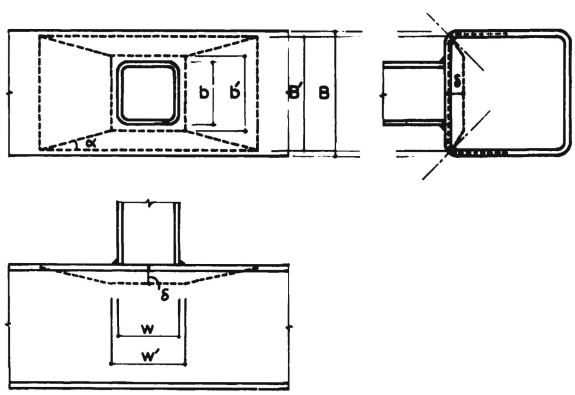


FIG.7.-ASSUMED YIELD-LINES

modified width of chord flange; b' = b+2s = modified width of brace flange, s = size of fillet weld; and w' = w+2s = modified depth of brace web. Eq.2 is nondimensionalized by introducing a fictious load $P_o$ as follows:

$$\frac{P_{fy}}{P_o} = \sqrt{\frac{\beta}{\beta-1}} + \frac{\beta'}{2(\beta-1)} \qquad \cdots\cdots\cdots (3)$$

in which $\beta = B'/b'$; $\beta' = w'/b'$ (= 1.0 when the brace member is the square section); and $P_o = 16m_p$ = yield load of chord flange when a point load is applied at the center of chord flange, and is derived by introducing b' = w' = 0 in Eq.2.

Predicted values by Eq.3 is compared with test results with square brace sections in Fig.8. Test results of M1 and M4 and M5-types of specimens are plotted in addition to those of M2-type of specimens (M3-type of specimens are eliminated, because the local buckling of brace member belongs essentially to another category).

With respect to the M2-type of specimens, the correlation between the predicted values and measured yield loads is fairly good.

As for M1 and M4-types of specimens, test results can not be explained by Eq.3. Especially it should be noted that these plotts for M1 and M4-types of specimens are of maximum strength and can not be compared with Eq.3 which predict the yield load. And it suggests that the parameter B'/b' (similar to eccentricity e) is not the only parameter influential to the strengths of M1 and M4-types of specimens.

The critical ratio of $\beta = B'/b'$ for which Eq.3 is applicable seems to be about 1.20. This value coincides with the eccentricity e (= 30mm) obtained from the discussion of the relation between failure mode and geometry in Fig.6 which is also shown in Fig.8.

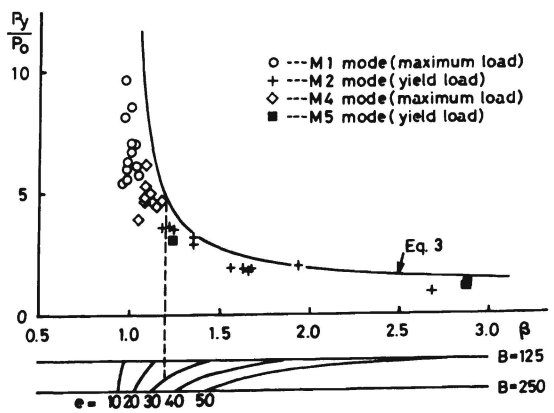


FIG.8.-APPLICABILITY OF YIELD-LINE THEORY

## 6.3. WEB-CRIPPLING STRENGTH OF CHORD WEBS

Theoretical research on M1-type failure mode (web-crippling of chord webs) is very few.

Recently Szlendak and Bródka (5) presented a theoretical prediction of the web-crippling strength of T-joints using a simple kinematically admissible model for b/B = 1.0, but test results with large b/B-ratio (larger than 0.80) obtained in the present study were found to locate far below that prediction as shown in Fig.9. This serious discrepancy seems to have come from the fact that the secondary moment caused by axial force and deflection of chord web was not considered in the strength evaluation of the chord web.

Web-crippling of chord members can be simulated by eccentrically loaded

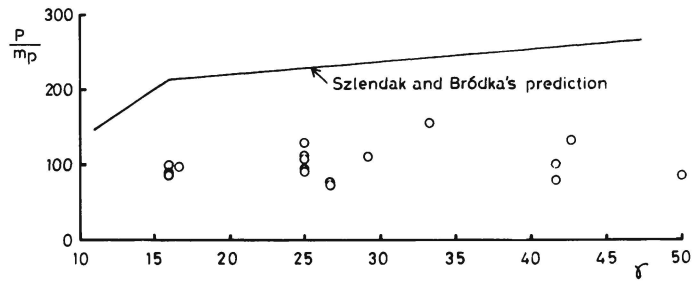


FIG.9.-COMPARISON OF TEST RESULTS AND SZLENDAK AND BRÓDKA'S PREDICTION

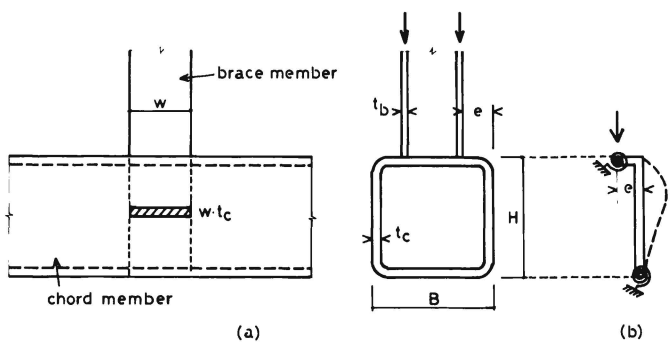


FIG.10.-BEAM-COLUMN ANALOGY

columns as shown in Fig.10(b), and parameters $\gamma = H/t_c$ and e (or b/B) must give the important influence on the strength of the system. The influence of these parameters on the web-crippling strength is observed in Fig.11, where the web-crippling strength $P_m$ is nondimensionalized by $P_w$ (= $2wt_c\sigma_y$ = the yield strength of two plates with width of w and thickness of $t_c$ as shown in Fig.10(a)). The specimens whose braces are not made of square hollow section members are excluded in the figure.

From Fig.11, it can be seen that the difference between M1 and M4 is not significant, and that it may be possible to make an empirical formula with the similar form to that of eccentrically loaded column.

Further investigation and analysis of this problem is underway.

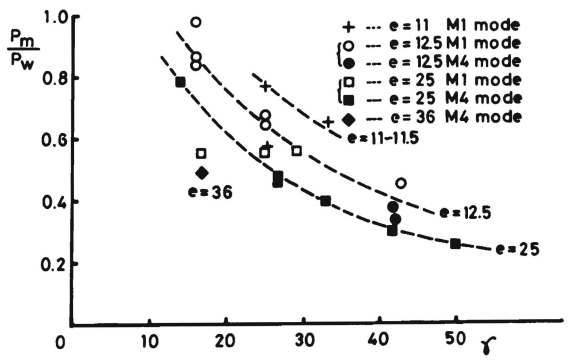


Fig.11.-WEB-CRIPPLING STRENGTH OF CHORD MEMBERS

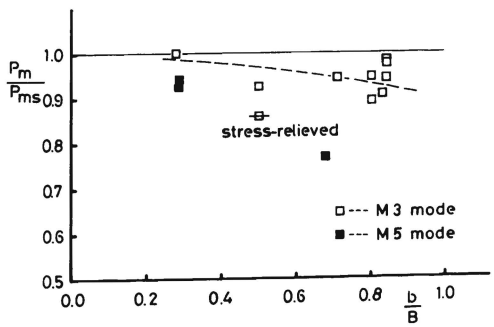


FIG.12.-LOCAL BUCKLING STRENGTH OF BRACE MEMBERS

## 6.4. LOCAL BUCKLING STRENGTH OF BRACE MEMBER

Brace members in T-joints are supported by the flanges of chord members at one end. Since the flexural rigidities of a chord flanges are different each other in longitudinal and transverse directions, axial stresses distribution in two perpendicular walls of the brace member will be influenced by this different supporting condition.

The influence of the supporting condition on the local buckling strength of brace members is observed for M3 and M5-types of specimens in Fig.12. In this figure, the ratio $P_m/P_{ms}$ is taken in vertical axis and b/B-ratio is taken in horizontal axis, where $P_m$ is the measured maximum strength of brace members and $P_{ms}$ is the corresponding buckling load of stub columns. The adverse effect caused by anisotropic support increase with the increase of b/B-ratio. But for M3-type of specimens, the reduction from the stub column strength is at most 10%. For M5-type of specimens and for stress-relieved specimens, the effect of b/B-ratio seems to be much more considerable.

## 6.5. EFFECT OF STRESS-RELIEVING

To investigate the effect of cold-forming, a few specimens (see Table 1) are fabricated from stress-relieved rectangular hollow section members. The condition of stress-relieving is 560°C for one hour.

The comparison of test results between cold-formed and stress-relieved specimens is shown in Table 4 (which is already included in Table 3). No change of failure mode had occured, and for all failure mode of specimens, the maximum or yield loads had reduced by applying the stress-relieving. This reduction seems to be attributed mainly to the reduction of material properties (see the reduction of yield stress of tensile coupon in Table 2).

TABLE 4.-COMPARISON OF STRENGTH BETWEEN COLD-FORMED AND STRESS-RELIEVED SPECIMENS

| Cold-formed | | | | Stress-relieved | | | |
|---|---|---|---|---|---|---|---|
| Specimen number | $P_m$ kN | $P_y$ kN | Failure mode | Specimen number | $P_m$ kN | $P_y$ kN | Failure mode |
| (1) | (2) | (3) | (4) | (5) | (6) | (7) | (8) |
| 1 | 565 | - | M1 | 1' | 541 | - | M1 |
| 2 | 353 | - | M1 | 2' | 332 | - | M1 |
| 17 | 248* | 154 | M2 | 17' | 223* | 153 | M2 |
| 33 | 398 | 247 | M2 | 33' | 356 | 230 | M2 |
| 36 | 706* | 668 | M4 | 36' | 619 | 598 | M4 |
| 41 | 208 | - | M3 | 41' | 200 | - | M3 |

## 7. CONCLUSIONS

In a series of tests on welded T-joints made of rectangular or square hollow sections, three dominating failure modes were clearly recognized, they are M1 (web-crippling of chord webs), M2 (flexural failure of chord flanges) and M3 (local buckling of brace members). Corresponding to these three failure modes, the load-deformation curve of each category of specimens had also shown its distinguished feature as shown in Fig.5.

The main findings from this research are:

1. As for M1-type of specimens, it was found that e (or b/B) and $\gamma$ are the most influential parameters to their web-crippling strength. An empirical relation between the strength and these parameters was clearly recognized as seen in Fig.11. Further investigation and analysis on this problem is underway.
2. As for M2-type of specimens of which some informations are already available, the strength and behavior seems to be able to be explained in the light of the yield-line theory (see Fig.8).
3. The critical boundary of the geometry of specimens at which the failure mode transfers from M1 to M2 was found to be about e = 30mm or B'/b' = 1.2 (see Figs.6 and 8).
4. Due to an anisotropy of the supporting flange of chord members, the total buckling strength of brace members had shown slight reduction from the corresponding buckling strength obtained from the stub column test. Though the amount of reduction depends upon the b/B-ratio, it may account for at most 10%.
5. To investigate the effect of cold-forming, a few specimens were fabricated from stress-relieved rectangular hollow section members and the strength was compared with that of corresponding cold-formed specimens. For all specimens tested, the yield or the maximum strength of stress-relieved specimens was a bit smaller than that of corresponding cold-formed specimens. But the amount of reduction was at most 10%, and it seems to be not substantial from the statistical view point. This reduction seems to be attributed mainly to the reduction of material properties due to stress-relieving (annealing).

## ACKNOWLEDGMENT

This investigation was sponsored by CIDECT (Comitée International pour le Développment et l'Etude de la Construction Tubulaire). The opinions, findings, and conclusions expressed in this paper are those of the writers and not necessarily of the sponsors.

## APPENDIX.--REFERENCES

1. Chandrakeerthy,S.R.De S.,"Structural behaviour related to stress analysis of joints in cold-formed square hollow sections,vol.1.,"Dept. of Civil Engrg., Univ. of Sheffield, Sept. 1973.
2. Johansen,K.W.,"Yield-line theory," Cement and concrete association, 52 Grosvenor Gardens, London SW1, 1962.

3. Kato,B. and Nishiyama,I.,"The static strength of R.R-Joints with large b/B-ratio," Dept. of Architecture, Faculty of Engrg., Univ. of Tokyo, Japan, Aug. 1979.
4. Packer,J.A.,"Theoretical behaviour and analysis of welded steel joints with R.H.S. chords (final report)," Dept. of Civil Engrg., Univ. of Nottingham, Oct. 1978. CIDECT Report 5U-78/19.
5. Szlendak,J. and Bródka,J.,"Ultimate load of X and T-joints in rectangular hollow section for $\xi = 1$," I.I.W. Polish Delegation, Jan. 1980.
6. Wardenier,J. and Koning de C.H.M.,"Investigation into the static strength of welded lattice girder joints in structural hollow sections. Part I: Rectangular hollow sections," Stevin Report nr.6-76-4, CIDECT Report nr.76-12-[5Q].

## APPENDIX.--NOTATION

The following symbols are used in this paper:

$A$ = sectional area of rectangular hollow section;
$B$ = flange width of chord member;
$b$ = flange width of brace member;
$B' = B-(4-1.5\sqrt{2})t_c$ = modified flange width of chord member;
$b' = b+2s$ = modified flange width of brace member;
$D_1, D_2, D_3, D_4$ = the readings of the deformation dials;
$e = (B-b)/2$ = eccentricity;
$H$ = web depth of chord member;
$h$ = length of brace member;
$L$ = span length of chord member;
$M1, M2, M3, M4, M5$ = failure modes;
$m_p = t_c^2\sigma_y/4$ = full plastic moment of flange plate per unit width;
$P$ = applied load on the top of brace member;
$P_{fy}$ = theoretical yield strength of chord flange;
$P_m$ = experimental maximum strength of T-joint specimen;
$P_{ms}$ = experimental maximum load of stub column;
$P_o = 16m_p$;
$P_w = 2wt_c\sigma_y$;
$P_y$ = experimental yield strength of T-joint specimen;
$P_{ys}$ = experimental yield load of stub column;
$r = 2t_c$ = radius of curvature on the outer surface of the rectangular hollow section;
$s$ = size of fillet weld;
$t_b$ = wall thickness of brace member;
$t_c$ = wall thickness of chord member;
$w$ = web depth of brace member;
$w' = w+2s$ = modified web depth of brace member;
$\beta = B'/b'$;
$\beta' = w'/b'$;
$\Delta = (D_1+D_2+D_3+D_4)/2$;
$\sigma_{ms} = P_{ms}/A$ = experimental maximum stress of stub column;
$\sigma_T$ = tensile strength of test coupon (in tension);
$\sigma_{TJIS}$ = specified minimum tensile stress ($420N/mm^2$);
$\sigma_y$ = yield stress of test coupon (in tension);
$\sigma_{YJIS}$ = specified minimum yield stress ($235N/mm^2$);
$\sigma_{ys} = P_{ys}/A$ = experimental yield stress of stub column; and
$\gamma = H/t_c$.

SUMMARY

Static strength of welded T-joints made of cold-formed rectangular hollow sections was experimentally investigated.

Test results were compared with yield-line theory and the possible adaptation limit was clarified. The effect of cold-working or residual stresses on the joint strength was clarified to be negligible.